Chemosphere 343 (2023) 140244

Contents lists available at ScienceDirect

Chemosphere

journal homepage: www.elsevier.com/locate/chemosphere

Unlocking the hidden value of industrial by-products: Optimisation of bioleaching to extract metals from basic oxygen steelmaking dust and goethite

Ipek Tezyapar Kara, Nuannat Simmons, Stuart T. Wagland, Frederic Coulon *

Cranfield University, School of Water, Energy and Environment, Cranfield, MK43 0AL, UK

HIGHLIGHTS

- Bioaching was evaluated using Taguchi L9 orthogonal array design for metallurgical by-products.
- Optimum condition to leach selected metals form BOS-D and goethite was defined.
- The most influencing parameters were found as solid concentration followed by pH.

GRAPHICAL ABSTRACT

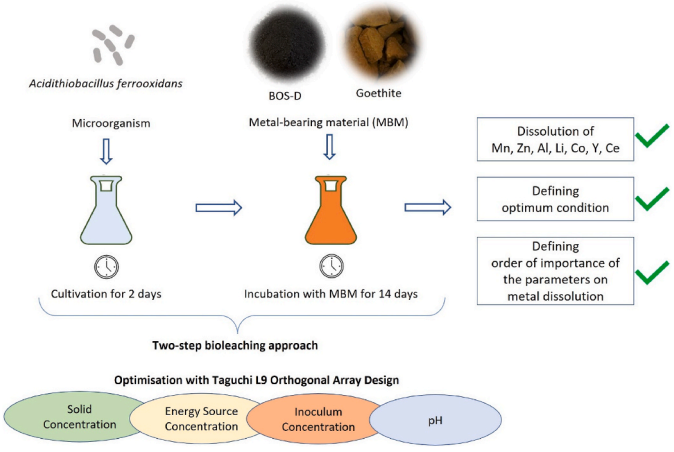

ARTICLE INFO

Handling editor: Y Yeomin Yoon

Keywords:
Acidithiobacillus ferrooxidans
Bioleaching
Metallurgical by-products
Metal dissolution
Biohydrometallurgy

ABSTRACT

In this study, the potential of bioleaching to extract valuable metals from industrial by-products, specifically basic oxygen steelmaking dust (BOS-D) and goethite was investigated. These materials are typically discarded due to their high zinc content and lack of efficient regeneration processes. By using *Acidithiobacillus ferrooxidans*, successful bioleaching of various metals, including heavy metals, critical metals, and rare earth elements was achieved. The Taguchi orthogonal array design was used to optimise the bioleaching process, considering four variables at three different levels. After 14 days, the highest metal extraction for the BOS-D (11.2 mg Zn/g, 3.2 mg Mn/g, 1.6 mg Al/g, 0.0013 mg Y/g, and 0.0026 mg Ce/g) was achieved at 1% solid concentration, 1% energy source concentration, 1% inoculum concentration, and pH 1.5. For goethite, the optimal conditions were 1% solid concentration, 4% energy source concentration, 10% inoculum concentration, and pH 2 resulting in a extraction of 26.6 mg Zn/g, 2.1 mg/g Mn, 1.8 mg Al/g, 0.01 mg Co/g, 0.0022 mg Y/g. These findings are significant, as they demonstrate the potential to extract valuable metals from previously discarded industrial by-products. The extraction of such metals can have substantial economic and environmental implications, while

* Corresponding author.
E-mail address: f.coulon@cranfield.ac.uk (F. Coulon).

https://doi.org/10.1016/j.chemosphere.2023.140244
Received 28 June 2023; Received in revised form 19 September 2023; Accepted 20 September 2023
Available online 25 September 2023

simultaneously reducing waste in the metallurgical industry. Furthermore, the preservation of initial concentration of iron in both BOS-D and goethite residues represents a significant step towards implementing more sustainable industrial practices.

1. Introduction

Metallurgical by-products including basic oxygen steelmaking dust (BOS-D), and goethite are often considered as waste and stockpiled on former and current metallurgical sites, despite containing valuable metals such as manganese (Mn), lead (Pb), aluminum (Al), critical metals like lithium (Li) and cobalt (Co), and rare earth elements (REE) such as yttrium (Y) and cerium (Ce) (Binnemans et al., 2020; Hoeber and Steinlechner, 2021; Ma, 2008). Approximately, 20 kg of BOS-D is produced for per ton of liquid steel (Stewart and Barron, 2020; Binnemans et al., 2020), and 250 kg goethite is produced from per ton of ore (Rodriguez et al., 2020). Unfortunately, the high zinc content in metallurgical by-products, such as BOS-D (>10 g/kg) and goethite (ranging between 50 and 100 g/kg), hinders their potential for reuse (Binnemans et al., 2020; Ma, 2016; Di Maria and Van Acker, 2018). Recovering metals from these secondary resources is not only critical for sustainable development but also for reducing environmental risks posed by historic contaminated sites (Di Maria and Van Acker, 2018; Riley et al., 2020). However, the current pyro- and hydro-metallurgical methods for extracting metals from these by-products are not economically feasible due to low extraction yields, metal loss, and the generation of aqueous waste streams that require additional treatment (Binnemans et al., 2020; Di Maria and Van Acker, 2018).

Bioleaching, also known as biomining, is a promising eco-friendly and cost-effective alternative to traditional hydro- and pyro-metallurgical process. It can be operated at low temperature (25–35 °C) and atmospheric pressure, producing no harmful gas emissions. The process involves the use of bacteria and fungi and their metabolites, to solubilise metals from metal-bearing materials (MBM). Bioleaching can occur directly, where microorganisms attach to the MBM surface to solubilise metals; indirectly where the metabolites react with the MBM, or cooperatively, where the two phenomena occur simultaneously. Acidophiles are the most commonly used microbial group, utilising ferrous iron and/or reduced sulphur compounds (S_8, $S_2O_3^{2-}$, H_2S) to generate leaching agents such as ferric iron (Fe^{+3}) and sulphuric acid (H_2SO_4). Metal dissolution from acidophiles form sulphide ores (Eqs. (1)–(3)) (Mishra et al., 2005; Srichandan et al., 2019), oxidic ores (Eq. (4)) (Abhilash and Pandey, 2013; Zare Tavakoli et al., 2017) and electronic wastes (Eqs. (5) and (6)) (Işıldar et al., 2016; Pourhossein and Mousavi, 2019).

$$2Fe^{2+} + 0.5O_2 + 2H^+ \xrightarrow{A.f.} 2Fe^{3+} + H_2O \quad (1)$$

$$FeS_2 + 6Fe^{3+} + 3H_2O \rightarrow S_2O_3^{2-} + 7Fe^{2+} + 6H^+ \quad (2)$$

$$S_2O_3^{2-} + 8Fe^{3+} + 5H_2O \rightarrow 2SO_4^{2-} + 8Fe^{2+} + 10H^+ \quad (3)$$

$$UO_2 + Fe_2(SO_4)_3 \rightarrow UO_2SO_4 + 2FeSO_4 \quad (4)$$

$$Cu^0 + 2Fe^{3+} \rightarrow 2Fe^{2+} + Cu^{2+} \quad (5)$$

$$Ni^0 + 2Fe^{3+} \rightarrow 2Fe^{2+} + Ni^{2+} \quad (6)$$

The bioleaching process performance is influenced by multiple parameters including pH, solid concentration (also termed as pulp density), energy source concentration, temperature, leaching time. Simultaneously optimising these parameters can enhance bioleaching efficiency (Niu et al., 2016). Several multivariable optimisation methods such as a central composite design (CCD), Box–Behnken, and Taguchi orthogonal array design have been used for bioleaching studies (Amiri et al., 2011a; Jalali et al., 2019; Mo et al., 2019; Nkulu et al., 2013). Compared to other experimental designs, the Taguchi method is advantageous because it requires fewer experiments to achieve optimal conditions. It uses orthogonal arrays to efficiently explore a large parameter space with a relatively small number of experiments, making it a cost-effective and time-saving method. In addition, the Taguchi method allows to evaluate simultaneously the relative importance of different parameters and to identify the optimal combination of parameter values that will produce the highest yield with the least variation. This is particularly useful in bioleaching studies where it is crucial to optimise the yield of metal extraction and minimise the variability of the process. In this study, leachability of metals from BOS-D and goethite using *Acidithiobacillus ferrooxidans* (*A. ferrooxidans*) was investigated. The influence of four factors including solid concentration, energy source concentration ($FeSO_4.7H_2O$ as a source of Fe^{2+}), inoculum concentration and pH was evaluated at three levels using Taguchi orthogonal array design. This study sheds light on the potential of bioleaching as a viable and sustainable alternative to conventional hydrometallurgical and pyrometallurgical processes. It highlights the positive impact of bioleaching on the leachability of certain metals, thus underscoring its potential as a promising technology for efficient and eco-friendly metal extraction.

2. Materials and methods

2.1. Characterisation of materials

A bulk mixture of BOS-D from a historical iron and steelwork plant stockpiled in Teesside, UK, was received in a large, sealed drum and stored at ambient temperature. Additionally, goethite, a mineral residue from zinc ore refining throughout a hydro-metallurgical process, was obtained from the Nyrstar plant in Auby, France and stored in a bucket at ambient temperature. Both samples were air-dried, ground, and sieved through a 2 mm mesh. The physical-chemical analysis results for BOS-D and goethite can be found in Supplementary Material (Fig. S1). Characterisation methods used have been previously described in Tezyapar Kara et al. (2022). To prepare the materials for bioleaching experiments, both materials were autoclaved for 15 min at 121 °C. The elemental composition of the autoclaved materials was determined using aqua regia digestion, with 1:3 ratio of nitric acid (HNO_3) and hydrochloric acid (HCl), followed by microwave digestion as described by Gutiérrez-Gutiérrez et al. (2015). Extracts were analysed with a PerkinElmer's NexION® Inductively Coupled Plasma Mass spectrometer (ICP-MS) using uranium (U) as internal standard as described Gutiérrez-Gutiérrez et al. (2015). Several standard solutions sourced from PerkinElmer for calibration were used: mercury ICP-MS standard, single ICP-MS standard for precious metals, single ICP-MS standard for As, Mo, Re, Sb, Si and single ICP-MS standards for the rest of the metals with the analyte concentration of 10 μg/ml. The mineral composition of both BOS-D and goethite was analysed using X-ray diffraction (XRD) using a Bruker D5005 diffractometer with a copper tube ($\lambda K\alpha = 0.154$ nm) (Kremser et al., 2022). The step size was 0.02° 2θ, the time per step was 1 s, the angular range was 10–90° 2θ, and the total scan duration was 67min. The data acquisition software used was Bruker XRD Commander, and the data processing software used was Bruker Diffrac.EVA. The surface morphology and elemental distribution of both BOS-D and goethite were examined through scanning electron microscopy (SEM) and energy-dispersive X-ray spectroscopy (EDS) analysis (TESCAN VEGA4) prior to and post-bioleaching.

2.2. Taguchi orthogonal array design

To assess the impact of various parameters on the dissolution of metals from BOS-D and goethite materials the Taguchi orthogonal array design L9 (3^4) was chosen. Details of the computational method of Taguchi array design are provided in Tang et al. (2016), Gu et al. (2017), Nkulu et al. (2013). This design involved optimising four parameters, including solid concentration (1, 5 and 10% w/v), energy source concentration (1%, 2% and 3% w/v for BOS-D optimisation and 2%, 3% and 4% w/v for goethite optimisation), inoculum concentration (1, 5 and 10% v/v) and pH (1.50, 1.75, and 2.00), in three different levels under 9 different conditions (Table 1). The range of parameters for optimisation was selected based on Tezyapar Kara et al. (2023) and Mo et al. (2019). For the bioleaching of oxidic BOS-D, an intermediate energy source concentration of 2.22% was chosen, in accordance with the findings of Chen et al. (2015) and Gomes et al. (2018). Additionally, for the bioleaching of goethite, we considered an energy source concentration of 4.44%, as supported by the research of Jensen and Webb (1995), Roy et al. (2021), and Zeng et al. (2013). The optimisation results were analysed using Minitab® 19.2020.1 (Eisapour et al., 2013). Based on these responses signal-to-noise ratios (S/N) were calculated using larger is better function (Eq. (7)) and optimum responses (Y_{opt}) (Eq. (8)) were predicted using Minitab (Awolusi et al., 2022; Nkulu et al., 2013).

$$SN_i = -10\,log_{10}\left(\frac{1}{m}\sum_{j=1}^{m}\frac{1}{y_{ij}^2}\right) \tag{7}$$

$$Y_{opt} = \frac{T}{n} + \left(A_i - \frac{T}{n}\left(B_j - \frac{T}{n}\right)\right) + \tag{8}$$

where y_{ij} is the response y_j at the level I, T/n is the mean of all the responses; and A_i, B_j, … are the means of the responses corresponding to the optimal conditions (Nkulu et al., 2013). Then, S/N values were used to define the order of importance of the parameters and the optimum level of the parameters. The difference of maximum and minimum S/N values for each parameter is called relative score (Δ) and larger relative score represents the most influencing parameter (Gu et al., 2017; Tang et al., 2016).

2.3. Batch bioleaching optimisation experiments

Actively growing culture of *A. ferrooxidans* (DSM 583) was sourced from the Leibniz Institute (DSMZ), Braunschweig (Germany). The culture was adapted to 5% (w/v) of BOS-D as detailed in Tezyapar Kara et al. (2022) . To adapt the culture to goethite material, the same procedure was used (results are not shown). As ORP did not reach ≥600 mV within seven days for 2.5% (w/v) solid concentration, acclimatised culture for 1% (w/v) was used for bioleaching of goethite (Muddanna and Baral, 2021). Adapted cultures were preserved in Erlenmeyer flasks with a concentration of 10% (v/v). These cultures were maintained in 90 ml of optimised 4.5 K salt medium at pH 1.75 at 30 °C at 150 rpm as described by Chen et al. (2015). Prior to their use in the batch optimisation experiment, the adapted cultures were sequentially cultivated for 2 days on two separate occasions. Following the 2 days of cultivation, the pH of the cultures was 2.04 for both BOS-D and goethite, while the ORP values were 637 mV and 628 mV forBOS-D and goethite, respectively. The adapted cultures were then utilised in 250 ml batch optimisation experiments (Table 1). To begin with, three different growth media were prepared based on the desired ferrous iron concentration, as energy source concentration is an optimisation parameter. The optimised growth media consist of modified basal salt medium (MBSM) and a ferrous iron solution. MBSM was prepared by adding 2 g of $(NH_4)_2SO_4$, 0.25 g of K_2HPO_4, 0.25 g of $MgSO_4{\cdot}7H_2O$, 0.10 g of KCl and 0.01 g of $Ca(NO_3)_2$–700 ml of deionised water (Chen et al., 2015). The ferrous iron solution was prepared by adding varying amounts of $FeSO_4.7H_2O$, based on the optimisation level, to 300 ml deionised water. For BOS-D, 11.1 g, 22.2 g and 33.33 g $FeSO_4.7H_2O$ was used to obtain 2.22, 4.44 and 6.66 g/L Fe^{+2} in the medium, respectively. Both solutions were adjusted at pH 2.00 using 5 M H_2SO_4. After pH adjustment, MBSM was autoclaved at 121 °C for 15 min and the ferrous iron solution was filtered using 0.2 μm Millipore filter. The two solutions were then mixed to get the growth medium with the desired ferrous iron concentration (Table 1, parameter B). A two-step bioleaching approach was employed for this study (Amiri et al., 2011b). In the first step, the growth media were placed into 250 ml flasks, and the pH was adjusted to the different levels (Table 1, parameter D). Before inoculation, an equal amount of growth medium volume was discarded from the flask to create volume for inoculum. The flasks were inoculated with different concentrations (Table 1, parameter C) and incubated at 30 °C on an orbital shaker at 150 rpm. Bioleaching experiments were performed in triplicate for BOS-D and in duplicate for goethite. Abiotic control experiment was performed for 1% pulp density using 1.11% energy source for BOS-D and 2.22% energy source for goethite at pH 1.75. Acid control experiment was performed under same condition using only 5 M H_2SO_4 without $FeSO_4.7H_2O$. Control experiments were performed in duplicate. Throughout the experiment, the oxidation-reduction potential (ORP) and pH of the culture and control

Table 1
L9 (3^4) experimental design for both BOS-D and goethite materials.

Factor (parameter)		Variation level/real values					
Material		BOS-D			Goethite		
Level		1	2	3	1	2	3
A - Solid conc. % (w/v)		$A_1 = 1$	$A_2 = 5$	$A_3 = 10$	$A_1 = 1$	$A_2 = 5$	$A_3 = 10$
B - Energy source conc. % (w/v)		$B_1 = 1.11$	$B_2 = 2.22$	$B_3 = 3.33$	$B_1 = 2.22$	$B_2 = 3.33$	$B_3 = 4.44$
C - Inoculum conc. % (v/v)		$C_1 = 1$	$C_2 = 5$	$C_3 = 10$	$C_1 = 1$	$C_2 = 5$	$C_3 = 10$
D - pH		$D_1 = 1.50$	$D_2 = 1.75$	$D_3 = 2.00$	$D_1 = 1.50$	$D_2 = 1.75$	$D_3 = 2.00$
Conditions	Experimental scheme	Factors and their variation levels					
		BOS-D				Goethite			
		A	B	C	D	A	B	C	D
C1	$A_1B_1C_1D_1$	1	1.11	1	1.50	1	2.22	1	1.50
C2	$A_1B_2C_2D_2$	1	2.22	5	1.75	1	3.33	5	1.75
C3	$A_1B_3C_3D_3$	1	3.33	10	2.00	1	4.44	10	2.00
C4	$A_2B_1C_2D_3$	5	1.11	5	2.00	5	2.22	5	2.00
C5	$A_2B_2C_3D1$	5	2.22	10	1.50	5	3.33	10	1.50
C6	$A_2B_3C_1D_2$	5	3.33	1	1.75	5	4.44	1	1.75
C7	$A_3B_1C_3D_2$	10	1.11	10	1.75	10	2.22	10	1.75
C8	$A_3B_2C_1D_3$	10	2.22	1	2.00	10	3.33	1	2.00
C9	$A_3B_3C_2D_1$	10	3.33	5	1.50	10	4.44	5	1.50

were monitored on a daily basis, with pH being adjusted daily to the initial concentration, except for the goethite material where pH and ORP were only monitored and adjusted on the designated sampling days (days 0, 1, 3, 5, 8, 11, 16). In the second step, after 2 days of incubation, different amounts of materials were added into the flasks (Table 1, parameter A).

2.4. Analytical methods

The pH of the shake flask medium was measured using a Jenway 3540 pH meter by dipping the probe into flask and mixing the slurry after cleaning the probe with alcohol (70% v/v isopropanol) or biocleanse (5% v/v Teknon™ Biocleanse Concentrate) and rinsing it with autoclaved distilled water. The oxidation of Fe^{+2} to Fe^{+3} was used as an indicator of microbial growth and was monitored using an Ag/AgCl ORP probe (Roy et al., 2021). Leachate samples (2 ml) were collected and filtered through a 0.2 μm Millipore filter for further analysis on day 1, 3, 5, 8, 11, and 16. The concentration of Fe (II) was determined through titration with $K_2Cr_2O_7$ (Third et al., 2000), while metal concentration was determined by ICP-MS. The metal extraction yield was calculated using the following equation (Jalali et al., 2019):

$$R = m/m_0 x100 \quad (9)$$

where R is % metal extraction, m is soluble metal amount in the leachate (g) and m_0 is initial metal amount in autoclaved BOS-D and goethite.

3. Results and discussion

3.1. Characterisation of materials

In this study, the elemental composition of BOS dust and goethite, both subjected to autoclaving (Table 2) as well as their non-autoclaved counterparts (Table S1) were compared. The results showed that autoclaving goethite led to a loss of certain elements compared to BOS dust. While the focus of this study is not the effect of autoclaving, it is important to discuss how this process could potentially impact subsequent bioleaching. Autoclaving has been reported to cause weight loss in minerals due to the removal of volatile components or the breakdown of certain mineral phases (Hubau et al., 2020). In the case of goethite, autoclaving may lead to the loss of elements that are more susceptible to thermal degradation or volatilisation (Roberts et al., 2023). For elements with an initial concentration exceeding 6 mg/kg, the reduction in weight was minimal, remaining below 20% for both BOS-D and goethite. Conversely, for other elements, the weight loss could reach up to 50% when associated with goethite, whereas it was limited to 40% when interacting with BOS-D. (Table S1). This weight loss could affect the subsequent bioleaching process, as the availability and accessibility of metals for microbial activity may be altered. Furthermore, autoclaving can induce changes in the mineral structure, such as phase transformations or surface modifications (Yazici et al., 2009). These alterations can affect the reactivity of the mineral and its interaction with the microbial consortium responsible for bioleaching. For example, changes in surface area, mineral crystallinity, or the formation of new mineral phases may influence the attachment of microorganisms and their ability to access the mineral surface for bioleaching (Jenneman et al., 1986). It is worth noting that the specific effects of autoclaving on subsequent bioleaching can vary depending on the mineral composition, temperature, pressure, and duration of autoclaving. The impact may also differ for different microorganisms involved in the bioleaching process. Therefore, further investigations are necessary to comprehensively understand the consequences of autoclaving on bioleaching efficiency and metal extraction.

For this bioleaching study, autoclaved materials were used to ensuring precise evaluation of the targeted microbial activity and metal leaching without interference from the native microorganisms (Faraji et al., 2018; Gomes et al., 2018). Both BOS-D and goethite were dominated by iron, zinc, lead, manganese, aluminium, and magnesium. The XRD analysis results (Fig. S2) further reveal that magnetite (Fe_3O_4) is the dominant mineral in both materials, which is consistent with previous studies (Hoeber and Steinlechner, 2021).

BOS-D also contained calcite, graphite, kamacite, and wustite, while goethite contained lautite, zinc titanium oxide, and corkite. The exact differences in composition and concentration of elements between the two materials are shown in Table 2. The pH values of BOS-D and goethite were 9.40 and 4.30, respectively. This revealed that to perform acidophilic bioleaching using *A. ferrooxidans* pH should be adjusted during bioleaching at 1.50–2.25.

The SEM-EDS analysis results of BOS-D and goethite reveal the presence of globular iron particles in BOS-D and fine aggregated particles in goethite (Fig. 1) which is in agreement with previous studies (Kelebek et al., 2004; Stewart et al., 2022); after bioleaching, morphological changes were observed, with increased visibility of spheroids in BOS-D and a reduction in the size of large agglomerates in both materials, as observed in Fig. 1c and f, along with the detection of Fe, Al, Mn, Pb, and Zn elements through EDS mapping (Tian et al., 2022).

Table 2
Elemental composition of the autoclaved BOS-D (n = 2) and goethite (n = 3).

Element	BOS-D		Goethite	
REE	mg/kg	RSD (%)	mg/kg	RSD (%)
Y	1.3	12	2.3	7
La	0	–	1.8	9
Ce	3.8	1	5.6	7
Pr	0.4	25	0.6	9
Nd	1.8	7	2.4	4
Sm	0.3	23	0.4	7
Eu	<LOD	–	0.08	28
Gd	0.3	22	0.4	8
Tb	<LOD	–	<LOD	–
Dy	0.2	54	0.4	5
Ho	<LOD	–	0.04	38
Er	0.1	52	0.2	8
Tm	<LOD	–	<LOD	–
Yb	0.1	74	0.2	11
Lu	<LOD	–	<LOD	–
Sc	<LOD	–	<LOD	–
Critical metals	mg/kg	RSD (%)	mg/kg	RSD (%)
Li	4	4	3.2	10
Co	10	3	9	1
Sb	12	5	697	6
Cu	127	1	**203667**	6
Heavy metals	mg/kg	RSD (%)	mg/kg	RSD (%)
Cr	157	4	223	7
Ni	59	2	34.1	6
Zn	**18300**	**8**	**61615**	**7**
As	16	12	**5157**	7
Cd	62	10	423	5
Hg	1.0	139	75	6
Pb	**1738**	**9**	**24800**	**7**
Others	mg/kg	RSD (%)	mg/kg	RSD (%)
Be	0.38	22	0.5357	52
B	24	2	<LOD	–
Mg	**5062**	**9**	513.7	7
Al	**2660**	**3**	**11164**	**7**
Si	<LOD	–	<LOD	–
V	51	1	41.1	6
Mn	**5870**	**4**	**1457**	**7**
Fe	**390500**	**6**	**162333**	**7**
Ga	13	2	224	7
Mo	7.3	6	71.3	6
Ba	54	7	30.6	35
Re	0.03	141	–	–

Bold ones represent most abundant elements. RSD: relative standard deviation; <LOD: below limit of detection.

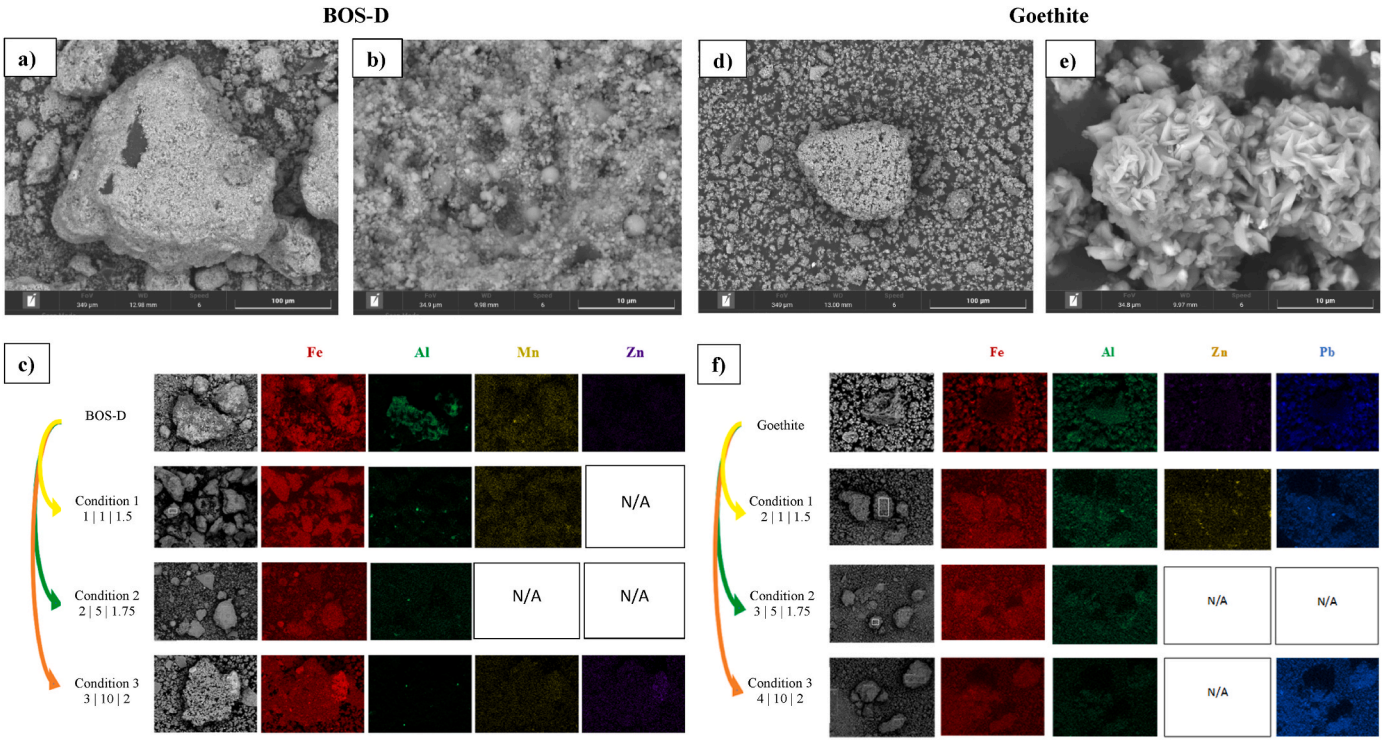

Fig. 1. SEM-EDS images of bioleaching residues of BOS-D and goethite under 1% (w/v) solid concentration. SEM result for BOS-D at 100 μm (a) and 10 μm (b); EDS result for BOS-D (c); SEM result for goethite at 100 μm (d) and 10 μm (e); EDS result for goethite (f). Series names represent the values of energy source concentration | inoculum concentration | pH.

3.2. Bioleaching experiment

ORP values and ferrous iron consumption during bioleaching of BOS-D are shown in Fig. 2. To facilitate the interpretation, results were grouped based on the tested solid concentration which are 1%, 5% and 10. In addition, the series names represent the values of "energy source concentration | inoculum concentration | pH". Before inoculation (Day 0), ORP values in all the flasks were around 300 (mV). On the Day 0 ferrous iron concentration were 2.22, 4.44 and 6.66 g/L in the flask that contain 1.11%, 2.22% and 3.33% (w/v) $FeSO_4.7H_2O$, respectively. First, flasks were inoculated with adopted cultures and cultivated for two days without BOS-D material. After two days of cultivation (Day 2), a linear increase in the ORP values (Fig. 2a, b, c) and a decrease in Fe^{2+} concentrations (Fig. 2d, e, f) were observed in all the flasks expect abiotic control. During acidophilic bioleaching ORP above 400 mV indicates there is a high concentration of Fe^{+3} and high bacterial growth (Rawlings and Johnson, 2007; Roy et al., 2021). According to Muddanna and Baral (2021), ORP ≥600 mV represents maximum ORP. ORP values in all the flasks were exceed the 400 mV in two days indicated that logarithmic phase of growth occurred (Roy et al., 2021). All flasks, except the flasks inoculated with 1% (v/v) culture and the flask with condition 3 | 5 | 1.5, reached maximum ORP (≥600 mV). After ORP measurement, BOS-D with different concentrations were added into the flasks. Sharp decrease in ORP (below 600 mV) had occurred instantly (Fig. 2a, b, c) and pH were increased (results not shown) due to alkali nature of the BOS-D (pH = 9.40). The pH was adjusted to the predefined values for each flask (Table 1) after BOS-D addition. On the next day (Day 3), ORP started to increase all the flasks that contain 1% (w/v) solid concentration and two of them reached out 600 mV again (Fig. 2a). ORP values of the rest of the flasks were below 570 mV. Following days all flasks were shown increasing trend until different times. Supportively, ferrous iron concentration followed a decreasing trend showing ferrous iron consumption by A. ferrooxidans (Fig. 2d, e, f). After Day 10, ORP values were in a downward trend for all the flasks until the end of the experiment (Day 16). Similarly, the ORP values and ferrous iron consumption during bioleaching of goethite are shown in Fig. 3. Results were grouped based on the tested solid concentration which are 1%, 5% and 10 to facilitate the interpretation, and the series names represent the values of "energy source concentration | inoculum concentration | pH". Before inoculation (Day 0), ORP values in all flasks were around 300 (mV). Besides, ferrous iron concentrations were 4.44, 6.66 and 8.88 g/L in the flask that contain 2.22%, 3.33% and 4.44% (w/v) FeSO4.7H2O, respectively. First, flasks were inoculated with adopted cultures and cultivated for two days without goethite. After two days of cultivation (Day 2), a linear increase in the ORP values (Fig. 3a, b, c) and a decrease in Fe2+ concentrations (Fig. 3d, e, f) were observed in all the flasks expect abiotic control. All flasks, except the flasks have 4.44% (w/v) energy source and the flask with condition 3 | 1 | 2, reached maximum ORP (≥600 mV) (Day 2). After the ORP measurement, goethite with different concentrations were added into the flasks. Sharp decrease in ORP had occurred instantly (Fig. 3a, b, c). As a following step, the pH was adjusted to the predefined values for each flask (Table 1) after the goethite addition. An increase in the ORP values were observed following days for the flasks that contain 1% (w/v) goethite and reached the maximum ORP (≥600 mV) by the end of the experiment (Fig. 3a). Flasks that contain 5% and 10% goethite also showed increase in ORP indicating that bacterial activity was continuing. The cumulative acid consumption during the experiment is illustrated in Fig. S3, and it is evident that BOS-D required 2 to 6 times more acid compared to goethite to maintain the desired pH, primarily due to its higher initial pH of 9.40 in contrast to goethite's pH of 4.30.

This discrepancy can be attributed to BOS-D significantly containing higher Mg element content (5062 mg/kg) compared to goethite (514 mg/kg), which contributes to an increase in pH during bioleaching (Chen et al., 2015). Furthermore, it was observed that acid consumption increased with an increase in solid concentration, as expected. The acid consumption also increased when the maintained pH value decreased from 2.00 to 1.50 for the same solid concentration.

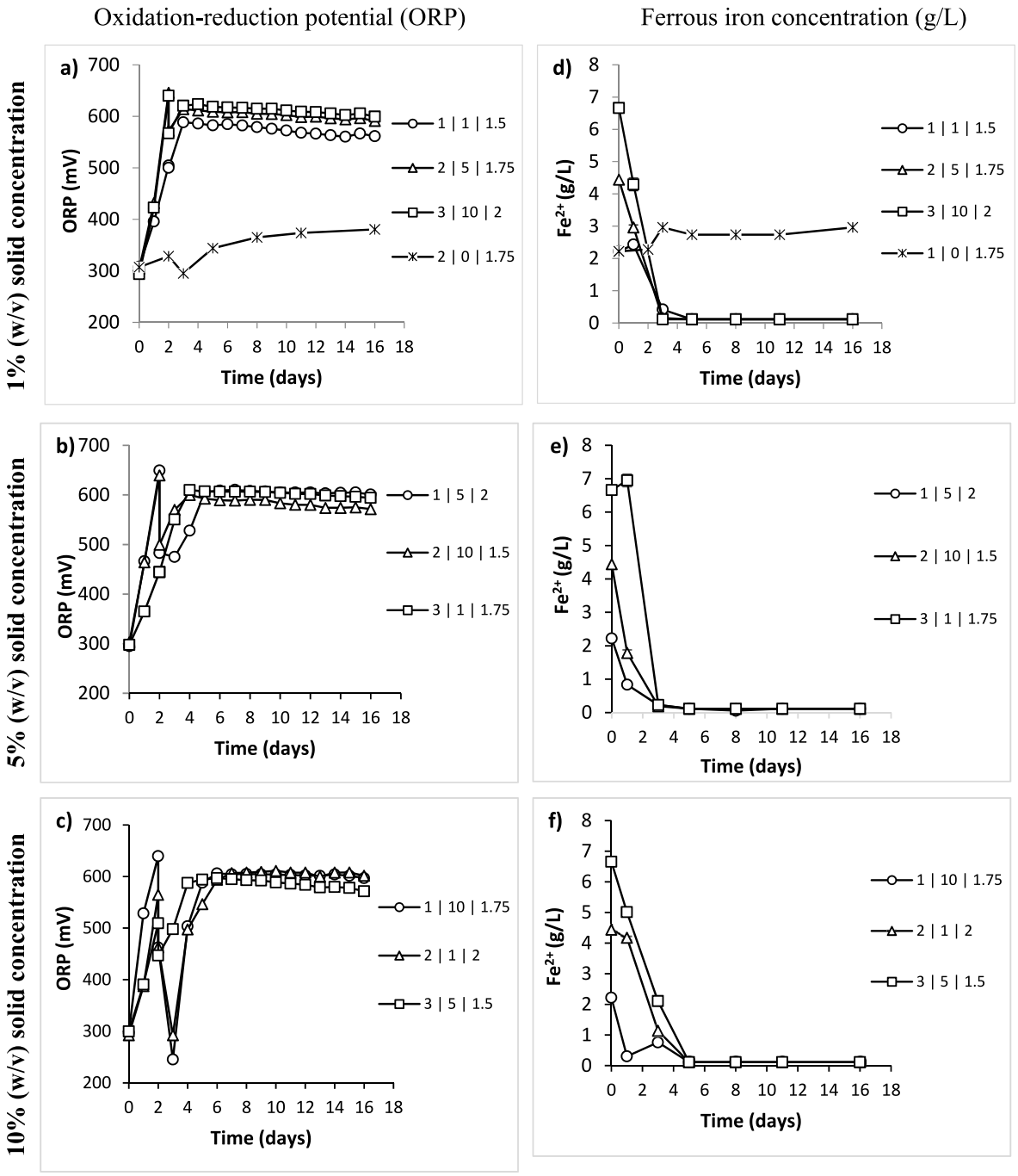

Fig. 2. Evolution of the ORP values (mV) and ferrous iron concentration (g/L) of BOS-D overtime (series names represent the values of energy source concentration | inoculum concentration | pH. n = 3; RSD for all elements ≤20%).

3.3. Taguchi statistical analysis

A comprehensive overview of the experimental setups and the average bioleaching yields (%) for each parameter studied, namely solid concentration, energy source concentration, inoculum concentration, and pH, individually evaluated for Mn, Zn, Pb, Al, Li, Co, Y, and Ce are summarised for BOS-D and goethite in Tables S2 and S3, respectively. The metals were categorised into three groups: the most abundant metals, critical metals, and rare earth elements (REEs).

3.3.1. Most abundant metals

For the bioleaching of Zn, Mn, and Al the calculated means of S/N ratios, relative scores (Δ), optimal level for each factor are presented in Table 3. Dissolution of Zn from BO-P was most affected by the energy source concentration (Δ = 1.12), followed by solid concentration (Δ = 0.82), pH (Δ = 0.69), and inoculum concentration (Δ = 0.58). On the other hand, for dissolution of Zn from goethite solid concentration appeared as the most influenced factor (Δ = 2.19) followed by pH (Δ = 1.08), inoculum rate (Δ = 0.57) and energy source concentration (Δ = 0.41).

Optimum experimental scheme for maximum dissolution of Zn from BOS-D was corresponded to $A_1B_1C_1D_3$ which is 1% solid concentration, 1% energy source concentration, 1% inoculum concentration and pH 2.00. For goethite, optimum experimental scheme was defined as $A_1B_3C_3D_2$ which indicated as follows 1% solid concentration, 4% energy source concentration, 10% inoculum concentration and pH 1.75.

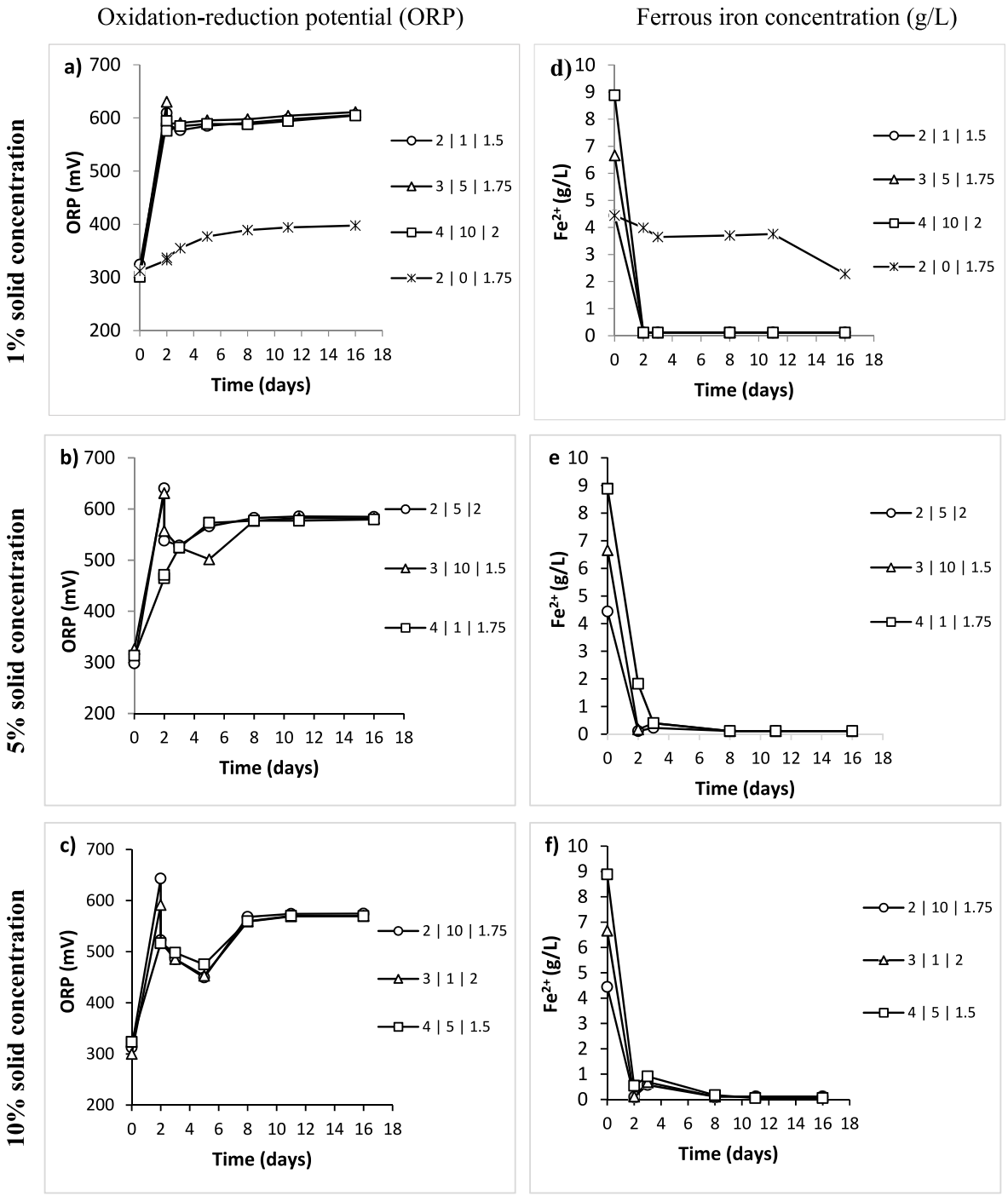

Fig. 3. Evolution of the ORP values (mV) and ferrous iron concentration (g/L) of goethite over time (series names represent the values of energy source concentration | inoculum concentration | pH. n = 2; RSD for all elements ≤20%).

Taguchi analyses predicted 64.3% and 44.4% of Zn dissolution from BOS-D and goethite, respectively, by using optimum experimental schemes.

For the manganese bioleaching solid concentration was the most influenced parameter for both BOS-D (Δ = 1.43) and goethite (Δ = 9.59). This factor followed by different parameters, yet inoculum concentration appeared as the less effective parameter for both. Taguchi analysis predicted that Mn extraction will increase 3% if optimum condition applies for Mn extraction from BOS-D. For Al dissolution, pH was the most affected parameter for both BOS-D (Δ = 1.64) and goethite (Δ = 1.56). Optimum experimental schemes were showed up as $A_2B_1C_1D_1$ for BOS-D and $A_3B_1C_1D_1$ for goethite. Pb did not involve Taguchi analysis due to Pb dissolution (13%) was only observed in $A_1B_1C_1D_1$, corresponding to: 1% solid concentration, 1% energy source concentration, 1% inoculum concentration and pH 1.50.

3.3.2. *Critical metals*

Lithium and cobalt were selected as critical metals to be investigated using Taguchi statistical analysis (Table 3). Overall, solid concentration was appeared as most influencing factor with 1% (w/v) optimum value for both BOS-D and goethite. This followed by different parameters and optimum values. For example, for Li dissolution from BOS-D, the second important factor was energy source concentration (Δ = 3.74) followed by inoculum concentration (Δ = 2.04). On the other hand, pH was the

Table 3
Mean of S/N ratios for each factorial level; the left column belongs to BOS-D and right column belongs to goethite.

Most abundant metals										
Zn_{obs} = 61% (C1,C4), Zn_{pre} = 64%					Zn_{obs} = 43% (C3), Zn_{pre} = 44%					
Levels	Factors				Levels	Factors				
	SC	ESC	IC	pH		SC	ESC	IC	pH	
1	1% = 35.01	1% = 35.2	1% = 34.9	1.5 = 34.51	1	1% = 32.1	2% = 30.65	1% = 30.61	1.5 = 30.28	
2	5% = 34.7	2% = 34.62	5% = 34.67	1.75 = 34.35	2	5% = 30.67	3% = 30.97	5% = 30.61	1.75 = 31.36	
3	10% = 34.19	3% = 34.08	10% = 34.32	2 = 35.04	3	10% = 29.91	4% = 31.06	10% = 31.18	2 = 31.04	
Optimal level	**A_1 = 1%**	**B_1 = 1%**	**C_1 = 1%**	**D_3 = 2**	**Optimal level**	**A_1 = 1%**	**B_3 = 4%**	**C_3 = 10%**	**D_2 = 1.75**	
Δ	0.82	1.12	0.58	0.69	Δ	2.19	0.41	0.57	1.08	
Rank	2	1	4	3	Rank	1	4	3	2	
Mn_{obs} = 57% (C1), Mn_{pre} = 60%					Mn_{obs} = 100% (C2, C3), Mn_{pre} = 100%					
Levels	Factors				Levels	Factors				
	SC	ESC	IC	pH		SC	ESC	IC	pH	
1	1% = 34.73	1% = 34.01	1% = 34.06	1.5 = 33.49	1	1% = 39.55	2% = 32.88	1% = 34.28	1.5 = 33.7	
2	5% = 33.61	2% = 34.05	5% = 33.71	1.75 = 33.65	2	5% = 32.26	3% = 34.13	5% = 33.7	1.75 = 34.39	
3	10% = 33.3	3% = 33.58	10% = 33.87	2 = 34.51	3	10% = 29.96	4% = 34.75	10% = 33.78	2 = 33.68	
Optimal level	**A_1 = 1%**	**B_2 = 2%**	**C_1 = 1%**	**D_3 = 2**	**Optimal level**	**A_1 = 1%**	**B_3 = 4%**	**C_1 = 1%**	**D_2 = 1.75**	
Δ	1.43	0.48	0.34	1.02	Δ	9.59	1.87	0.57	0.71	
Rank	1	3	4	2	Rank	1	2	4	3	
Al_{obs} = 59% (C1), Al_{pre} = 61%					Al_{obs} = 24% (C9), Al_{pre} = 26%					
Levels	Factors				Levels	Factors				
	SC	ESC	IC	pH		SC	ESC	IC	pH	
1	1% = 33.23	1% = 34.04	1% = 33.99	1.5 = 34.32	1	1% = 25.7	2% = 26.63	1% = 26.69	1.5 = 27.19	
2	5% = 33.88	2% = 33.26	5% = 33.07	1.75 = 33.23	2	5% = 26.44	3% = 26.54	5% = 26.4	1.75 = 26.35	
3	10% = 33.12	3% = 32.93	10% = 33.18	2 = 32.68	3	10% = 27.03	4% = 26.01	10% = 26.08	2 = 25.63	
Optimal level	**A_2 = 5%**	**B_1 = 1%**	**C_1 = 1%**	**D_1 = 1.5**	**Optimal level**	**A_3 = 10%**	**B_1 = 1%**	**C_1 = 1%**	**D_1 = 1.5**	
Δ	0.77	1.1	0.92	1.64	Δ	1.33	0.62	0.61	1.56	
Rank	4	2	3	1	Rank	2	3	4	1	
Critical metals										
Li_{obs} = 92% (C1), Li_{pre} = 94%					Li_{obs} = 64% (C3), Li_{pre} = 64%					
Levels	Factors				Levels	Factors				
	SC	ESC	IC	pH		SC	ESC	IC	pH	
1	1% = 36.3	1% = 35.82	1% = 34.78	1.5 = 33.35	1	1% = 35.65	2% = 34.7	1% = 34.66	1.5 = 34.06	
2	5% = 32.91	2% = 33.07	5% = 33.46	1.75 = 32.94	2	5% = 34.63	3% = 34.55	5% = 34.6	1.75 = 34.9	
3	10% = 31.76	3% = 32.08	10% = 32.73	2 = 34.68	3	10% = 33.72	4% = 34.74	10% = 34.74	2 = 35.03	
Optimal level	**A_1 = 1%**	**B_1 = 1%**	**C_1 = 1%**	**D_3 = 2**	**Optimal level**	**A_1 = 1%**	**B_3 = 4%**	**C_3 = 10%**	**D_3 = 2**	
Δ	4.54	3.74	2.04	1.74	Δ	1.93	0.2	0.14	0.98	
Rank	1	2	3	4	Rank	1	3	4	2	
Co_{obs} = 54% (C2), Co_{pre} = 55%					Co_{obs} = 100% (C2, C3), Co_{pre} = 100%					
Levels	Factors				Levels	Factors				
	SC	ESC	IC	pH		SC	ESC	IC	pH	
1	1% = 33.68	1% = 32.02	1% = 31.93	1.5 = 31.24	1	1% = 38.72	2% = 30.22	1% = 31.9	1.5 = 31.17	
2	5% = 31.88	2% = 32.44	5% = 32.67	1.75 = 32.68	2	5% = 29.93	3% = 32.48	5% = 31.88	1.75 = 32.76	
3	10% = 31.24	3% = 32.34	10% = 32.2	2 = 32.88	3	10% = 27.19	4% = 33.14	10% = 32.06	2 = 31.92	
Optimal level	**A_1 = 1%**	**B_2 = 2%**	**C_2 = 5%**	**D_3 = 2**	**Optimal level**	**A_1 = 1%**	**B_3 = 4%**	**C_3 = 10%**	**D_2 = 1.75**	
Δ	2.43	0.42	0.73	1.65	Δ	11.53	2.92	0.18	1.6	
Rank	1	4	3	2	Rank	1	2	4	3	
REEs										
Y_{obs} = 100% (C5, C6), Y_{pre} = 100%					Y_{obs} = 100% (C1, C4, C7, C8), Y_{pre} = 100%					
Levels	Factors				Levels	Factors				
	SC	ESC	IC	pH		SC	ESC	IC	pH	
1	1% = 36.56	1% = 38.68	1% = 38.89	1.5 = 39.32	1	1% = 39.75	2% = 40	1% = 39.98	1.5 = 39.71	
2	5% = 39.61	2% = 38.78	5% = 38.83	1.75 = 38.97	2	5% = 39.91	3% = 39.8	5% = 39.65	1.75 = 39.86	
3	10% = 37.36	3% = 36.06	10% = 35.81	2 = 35.24	3	10% = 39.78	4% = 39.63	10% = 39.8	2 = 39.87	
Optimal level	**A_2 = 5%**	**B_2 = 2%**	**C_1 = 1%**	**D_1 = 1.5**	**Optimal level**	**A_2 = 5%**	**B_1 = 2%**	**C_1 = 1%**	**D_3 = 2**	
Δ	3.05	2.72	3.08	4.08	Δ	0.17	0.37	0.33	0.16	
Rank	3	4	2	1	Rank	3	1	2	4	
Ce_{obs} = 75.6% (C2), Ce_{pre} = 75%					Ce_{obs} = 14.8% (C6), Ce_{pre} = 15%					
Levels	Factors				Levels	Factors				
	SC	ESC	IC	pH		SC	ESC	IC	pH	
1	1% = 35.7	1% = 34.21	1% = 33.89	1.5 = 34.9	1	1% = 23.18	2% = 23.27	1% = 23.11	1.5 = 23.19	
2	5% = 34.4	2% = 34.5	5% = 34.71	1.75 = 34.87	2	5% = 23.36	3% = 23.06	5% = 23.15	1.75 = 23.24	
3	10% = 32.12	3% = 33.49	10% = 33.6	2 = 32.45	3	10% = 22.9	4% = 23.12	10% = 23.18	2 = 23.01	
Optimal level	**A_1 = 1%**	**B_2 = 2%**	**C_2 = 5%**	**D_1 = 1.5**	**Optimal level**	**A_2 = 5%**	**B_1 = 2%**	**C_3 = 10%**	**D_2 = 1.75**	
Δ	3.58	1.01	1.11	2.45	Δ	0.46	0.21	0.07	0.22	
Rank	1	4	3	2	Rank	1	3	4	2	

second important factor, followed by energy source concentration for bioleaching of Li from goethite. However, even the order of importance of the pH was different for dissolution of Li, optimum pH value was appeared as 2.00 for both bioleached materials.

3.3.3. REEs

Bioleaching of yttrium and cerium was further analysed as rare earth elements (Table 3). Results showed that the factor with the highest significant is solid concentration for dissolution of Ce followed by pH for

both BOS-D and goethite. Optimum experimental scheme for dissolution of Ce from BOS-D was $A_1B_2C_2D_1$ respectively to 1% solid concentration, 2% energy source concentration, 5% inoculum concentration and pH 1.50. For maximum Ce extraction from goethite experimental scheme defined as $A_2B_1C_3D_2$ which is 5% solid concentration, 2% energy source concentration, 10% inoculum concentration and pH 1.75.

Optimum energy source level which is 2% (w/v) was the same for Ce dissolution from both BOS-D and goethite. In terms of yttrium, complete dissolution was achieved both by bioleaching and acid leaching from both materials. Overall, based on the predicted results for individual metal extraction, an increase of more than 3% is not anticipated. However, the pH parameter emerged as the most crucial factor after solid concentration. Therefore, implementing automated monitoring and adjustment systems for pH during the bioleaching process could potentially enhance metal extraction rates.

3.4. Metal extraction potential of BOS-D and goethite

To compare bioleaching efficiency on shake flask Mn, Zn, Pb, Al, Li, Co, Y, Ce were selected due to some of them the most abundant metals, critical and rare earth elements. The extraction yields for metals that have the initial concentrations are lower than 1 mg/kg was not reported. After 14 days of bioleaching, both materials, highest metal dissolution was achieved using 1% (w/v) solid concentration. From BOS-D, highest metal extraction from majority of selected elements, Zn, Pb, Al, Li and Y, was achieved under the condition of 1% solid concentration, 1% energy source concentration, 1% inoculum concentration, and pH 1.50 ($A_1B_1C_1D_1$) (Fig. S4a and Table 4). Under this condition, 54% Mn, 61% Zn, 13% Pb, 59% Al, 92% Li, 40% Co, 99% Y and 67% Ce were dissolved from BOS-D. This percentages correspond to 3.2 mg Mn, 11.2 mg Zn, 0.2 mg Pb,1.6 mg Al, 0.004 mg Li, 0.004 mg Co, 0.0013 mg Y and 0.0026 mg Ce extraction. Overall, 0.005 mg of REE, 0.09 mg of critical metals, 11.5 mg of heavy metals and 4.8 mg other metals were extracted from 1 g of BOS-D (Table 4). Although bioleaching yield of Zn (61%) was lower than acid leaching (73%), more additional elements such as Li, Y and Ce were also extracted from BOS-D. This result indicates the benefit of bioleaching. Bioleaching provided higher metal dissolution than acid leaching for Pb, Al, Li, Co, Y and Ce. The reason is that Fe^{3+} contributed leaching of these metals additionally when compared to control that contains only sulphuric acid (Kremser et al., 2021). For example, Li and Co dissolution under the influence of the energy sources and the products of bacterial activity can be explained by Equation (10) (Moazzam et al., 2021).

$$2FeSO_4 + 2LiCoO_2 + 4H_2SO_4 \rightarrow Fe_2(SO_4)_3 + 2CoSO_4^{2+} + Li_2SO_4 + 4H_2O \quad (10)$$

For goethite, highest metal extraction from majority of selected elements, Mn, Zn, Li, and Co, was achieved under the condition of 1% solid concentration 1% solid concentration, 4% energy source concentration, 10% inoculum concentration, and pH 2.00 ($A_1B_3C_3D_3$) (Fig. S4b and Table 4). Under this condition 100% Mn, 43% Zn, 16% Al, 64% Li, 100% Co, 96% Y and 14% Ce were dissolved from goethite. This percentages correspond to 2.1 mg Mn, 26.6 mg Zn, 1.8 mg Al, 0.002 mg Li, 0.013 mg Co, 0.0022 mg Y and 0.0008 mg Ce extraction. Overall, 0.004 mg of REE, 15.71 mg of critical metals, 26.8 mg of heavy metals and 3.9 mg other metals were extracted from 1 g of goethite (Table 4).

Bioleaching demonstrated superior metal dissolution compared to acid leaching for Mn, Zn, Li, and Co. Additionally, all the iron was preserved in the residues of both BOS-D and goethite (results not presented). Further research is required to reduce the Zn content to less than 1% in order to utilise goethite and BOS-D as secondary iron resources in the steel-making industry. Further to this, the SEM-EDS analysis results (Fig. 1c and f) demonstrate notable morphological changes in both BOS-D and goethite after bioleaching. In the case of BOS-D, increased visibility of spheroids is observed, while both materials exhibit a reduction in the size of large agglomerates post-bioleaching. EDS mapping reveals the presence of Fe, Al, Mn, Pb, and Zn elements. Following the bioleaching process, the distribution of Al, Zn, and Mn decreased in both BOS-D and goethite. The findings align with the leaching results, confirming that bioleaching, under optimised conditions, facilitates enhanced Zn extraction (Tian et al., 2022).

Table 4
Amounts of extracted elements of elements after bioleaching from 1 g of BOS-D and goethite. n = 3 for BOS-D and n = 2 for goethite; SD for all elements ≤20%.

Element	BOS-D		Goethite	
	Bioleaching yield (%)	Amounts of extracted element (mg)	Bioleaching yield (%)	Amounts of extracted element (mg)
REE				
Y	99	0.0013	96	0.0022
La	–	–	3	0.0001
Ce	67	0.0026	14	0.0008
Nd	80	0.0014	21	0.0005
Total REE		**0.005**		**0.004**
Critical metals				
Li	92	0.004	64	0.002
Co	40	0.004	100	0.013
Sb	7	0.001	0	0.000
Cu	61	0.077	77	15.7
Total critical metals		**0.09**		**15.71**
Heavy metals				
Cr	15	0.0	17	0.0
Ni	23	0.0	48	0.0
Zn	61	11.2	43	26.6
Cd	100	0.1	49	0.2
Pb	13	0.2	0	0.0
Total heavy metals		**11.5**		**26.8**
Others				
Al	59	1.6	16	1.8
V	21	0.0	0	0.0
Mn	54	3.2	100	2.1
Ga	6	0.0	1	0.0
Ba	26	0.0	0	0.0
Total other metals		**4.8**		**3.9**
Total elements		**16.4**		**46.4**

3.5. Kinetics of batch bioleaching

For a liquid/solid reaction system, the reaction rate is usually controlled by three main process which are diffusion through the liquid film, diffusion through the product layer, the chemical-controlled reaction at the surface of the solid particles (Asghari et al., 2013; Mishra et al., 2008; Naseri et al., 2019). The shrinking core model (SCM) theory considers that the leaching process is controlled by one of these steps (Gharabaghi et al., 2013; Naseri et al., 2019; Pedram et al., 2020). In this study, the bioleaching kinetics were compared with the product layer diffusion theory and chemical reaction theory (Amiri et al., 2012; Gomes et al., 2018; Pathak et al., 2019; Wang et al., 2019). As the bioleaching solution was non-viscous, film diffusion as the rate-controlling step was disregarded (Pathak et al., 2019; Srichandan et al., 2020). The bioleaching yields of metals under the best overall conditions were used to calculate the kinetics: 1% energy source concentration, 1% inoculum concentration, and pH 1.50 for BOS-D, and 1% solid concentration, 4% energy source concentration, 10% inoculum concentration, and pH 2.00 for goethite (Fig. S5). The results obtained under the optimised conditions were used to fit two kinetic models: chemical reaction and product layer diffusion (Table S4). The correlations indicated that the dissolution of Zn, Li, Co, and Y from BOS-D aligned well with the chemical reaction model, suggesting the absence of a passivation layer on the surface of BOS-D or the presence of a porous layer that allowed the movement of leaching agents to reach the surface (Pathak et al., 2019). However, it's important to highlight that the pH range of 1.00–3.00 is conducive to the formation of jarosite, as indicated by Hou et al. (2015). Consequently, in the context of this research, it is highly probable that jarosite formation will take place. This occurrence could potentially account for the reduction in the extraction of Li and Y, hinting at the possibility of co-precipitation of dissolved elements with jarosite, in addition to any experimental errors (Fig. S5) (Opara et al., 2022; Pirsaheb et al., 2022). In the case of Al and Ce, the results suggested that the overall dissolution kinetics were likely controlled by the diffusion step (Rastegar et al., 2015). The bioleaching of Mn from both BOS-D and goethite, as well as Co from goethite, were influenced by both the chemical reaction and product layer diffusion. However, for goethite, most metals showed the opposite outcome. This discrepancy may be attributed to the daily acid adjustment performed during BOS-D bioleaching, while goethite bioleaching only involved sampling on specific days, leading to the formation of production or passivation layers such as jarosite, which slows down the leaching kinetics (Pathak et al., 2019). Regular acid addition can help prevent the formation of jarosite (Chen et al., 2015).

4. Conclusion

The study employed a L9 Taguchi orthogonal array design to evaluate the effects of solid concentration, energy source concentration, inoculum concentration, and pH on bioleaching. After a 14-day period, the highest metal extraction from BOS-D was achieved at 1% solid concentration, 1% energy source concentration, 1% inoculum concentration, and pH 1.50, while for goethite, the optimal condition was 1% solid concentration, 4% energy source concentration, 10% inoculum concentration, and pH 2.00. Solid concentration emerged as the most influential parameter, followed by pH. Regular monitoring and adjustment of pH can effectively prevent the formation of jarosite and enhance the bioleaching yield. The study successfully extracted metals such as Zn, Mn, Al, Li, Co, Y, and Ce from the materials. However, further research is necessary to reduce the Zn content to less than 1% in order to utilise goethite and BOS-D as secondary iron resources in the steelmaking industry.

Author contributions

Conceptualisation, I.T.K and F.C.; Formal analysis, I.T.K and N.S.; Writing, original draft preparation, I.T.K; Writing, review and editing, F. C. and S.T.W..; Supervision and feedback, F.C. and S.T.W.; Project administration, F.C., Funding acquisition, F.C. and S.T.W. All authors have read and agreed to the published version of the manuscript.

Declaration of competing interest

The authors declare that they have no known competing financial interests or personal relationships that could have appeared to influence the work reported in this paper.

Data availability

All the data supporting this study are included within the article and/or supporting materials.

Acknowledgements

This research was funded by the European Regional Development Fund as part of the Interreg Northwest Europe project "Regeneration of past metallurgical sites and deposits through innovative circularity for raw materials" (REGENERATIS) (NWE918). The authors would also like to thank Republic of Turkey Ministry of National Education ,Study Abroad Program, for sponsoring I. Tezyapar Kara. The authors also would like to thank Kristopher Bramley and Victoria Huntington for their help in the characterisation analysis.

Appendix A. Supplementary data

Supplementary data to this article can be found online at https://doi.org/10.1016/j.chemosphere.2023.140244.

References

Abhilash, Pandey, B.D., 2013. Microbially assisted leaching of uranium - a review. Miner. Process. Extr. Metall. Rev. 34, 81–113. https://doi.org/10.1080/08827508.2011.635731.

Amiri, F., Mousavi, S.M., Yaghmaei, S., 2011a. Enhancement of bioleaching of a spent Ni/Mo hydroprocessing catalyst by *Penicillium simplicissimum*. Separ. Purif. Technol. 80, 566–576. https://doi.org/10.1016/j.seppur.2011.06.012.

Amiri, F., Yaghmaei, S., Mousavi, S.M., 2011b. Bioleaching of tungsten-rich spent hydrocracking catalyst using *Penicillium simplicissimum*. Bioresour. Technol. 102, 1567–1573. https://doi.org/10.1016/j.biortech.2010.08.087.

Amiri, F., Mousavi, S.M., Yaghmaei, S., Barati, M., 2012. Bioleaching kinetics of a spent refinery catalyst using *Aspergillus Niger* at optimal conditions. Biochem. Eng. J. 67, 208–217. https://doi.org/10.1016/j.bej.2012.06.011.

Asghari, I., Mousavi, S.M., Amiri, F., Tavassoli, S., 2013. Bioleaching of spent refinery catalysts: a review. J. Ind. Eng. Chem. 19, 1069–1081. https://doi.org/10.1016/j.jiec.2012.12.005.

Awolusi, T., Taiwo, A., Aladegboye, O., Oguntayo, D., Akinkurolere, O., 2022. Optimisation of quinary blended supplementary cementitious material for eco-friendly paving unit using taguchi orthogonal array design. Mater. Today: Proc. 6, 2221–2227. https://doi.org/10.1016/j.matpr.2022.06.263.

Binnemans, K., Jones, P.T., Manjón Fernández, Á., Masaguer Torres, V., 2020. Hydrometallurgical processes for the recovery of metals from steel industry by-products: a critical review. J. Sustain. Metall. 6, 505–540. https://doi.org/10.1007/s40831-020-00306-2.

Chen, S., Yang, Y., Liu, C., Dong, F., Liu, B., 2015. Column bioleaching copper and its kinetics of waste printed circuit boards (WPCBs) by *Acidithiobacillus ferrooxidans*. Chemosphere 141, 162–168. https://doi.org/10.1016/j.chemosphere.2015.06.082.

Eisapour, M., Keshtkar, A., Moosavian, M.A., Rashidi, A., 2013. Bioleaching of uranium in batch stirred tank reactor: process optimization using Box–Behnken design. Ann. Nucl. Energy 54, 245–250. https://doi.org/10.1016/j.anucene.2012.11.006.

Faraji, F., Golmohammadzadeh, R., Rashchi, F., Alimardani, N., 2018. Fungal bioleaching of WPCBs using *Aspergillus niger*: observation, optimization and kinetics. J. Environ. Manag. 217, 775–787. https://doi.org/10.1016/j.jenvman.2018.04.043.

Gharabaghi, M., Irannajad, M., Azadmehr, A.R., 2013. Leaching kinetics of nickel extraction from hazardous waste by sulphuric acid and optimization dissolution conditions. Chem. Eng. Res. Des. 91, 325–331. https://doi.org/10.1016/j.cherd.2012.11.016.

Gomes, H.I., Funari, V., Mayes, W.M., Rogerson, M., Prior, T.J., 2018. Recovery of Al, Cr and V from steel slag by bioleaching: batch and column experiments. J. Environ. Manag. 222, 30–36. https://doi.org/10.1016/j.jenvman.2018.05.056.

Gu, W., Bai, J., Dong, B., Zhuang, X., Zhao, J., Zhang, C., Wang, J., Shih, K., 2017. Catalytic effect of graphene in bioleaching copper from waste printed circuit boards by *Acidithiobacillus ferrooxidans*. Hydrometallurgy 171, 172–178. https://doi.org/10.1016/j.hydromet.2017.05.012.

Gutiérrez-Gutiérrez, S.C., Coulon, F., Jiang, Y., Wagland, S., 2015. Rare earth elements and critical metal content of extracted landfilled material and potential recovery opportunities. Waste Manag. 42, 128–136. https://doi.org/10.1016/j.wasman.2015.04.024.

Hoeber, L., Steinlechner, S., 2021. A comprehensive review of processing strategies for iron precipitation residues from zinc hydrometallurgy. Clean. Eng. Technol. 4, 100214 https://doi.org/10.1016/j.clet.2021.100214.

Hou, Q., Fang, D., Liang, J., Zhou, L., 2015. Significance of Oxygen Supply in Jarosite Biosynthesis Promoted by Acidithiobacillus ferrooxidans 10, 1–12. https://doi.org/10.1371/journal.pone.0120966.

Hubau, A., Guezennec, A.G., Joulian, C., Falagán, C., Dew, D., Hudson-Edwards, K.A., 2020. Bioleaching to reprocess sulfidic polymetallic primary mining residues: determination of metal leaching mechanisms. Hydrometallurgy 197, 105484. https://doi.org/10.1016/j.hydromet.2020.105484.

Işıldar, A., van de Vossenberg, J., Rene, E.R., van Hullebusch, E.D., Lens, P.N.L., 2016. Two-step bioleaching of copper and gold from discarded printed circuit boards (PCB). Waste Manag. 57, 149–157. https://doi.org/10.1016/j.wasman.2015.11.033.

Jalali, F., Fakhari, J., Zolfaghari, A., 2019. Response surface modeling for lab-scale column bioleaching of low-grade uranium ore using a new isolated strain of Acidithiobacillus Ferridurans. Hydrometallurgy 185, 194–203. https://doi.org/10.1016/j.hydromet.2019.02.014.

Jenneman, G.E., McInerney, M.J., Crocker, M.E., Knapp, R.M., 1986. Effect of sterilization by dry heat or autoclaving on bacterial penetration through berea sandstone. Appl. Environ. Microbiol. 51, 39–43. https://doi.org/10.1128/aem.51.1.39-43.1986.

Jensen, A.B., Webb, C., 1995. Ferrous sulphate oxidation using thiobacillus ferrooxidans: a review. Process Biochem. 30, 225–236. https://doi.org/10.1016/0032-9592(95)85003-1.

Kelebek, S., Yörük, S., Davis, B., 2004. Characterization of basic oxygen furnace dust and zinc removal by acid leaching. Miner. Eng. 17, 285–291. https://doi.org/10.1016/j.mineng.2003.10.030.

Kremser, K., Thallner, S., Spiess, S., Kucera, J., Vaculovic, T., Višanský, D., Haberbauer, M., Guebitz, G.M., 2022. Bioleaching and selective precipitation for metal recovery from basic oxygen furnace slag. Processes 10, 576. https://doi.org/10.3390/pr10030576.

Kremser, K., Thallner, S., Strbik, D., Spiess, S., Kucera, J., Vaculovic, T., Vsiansky, D., Haberbauer, M., Mandl, M., Guebitz, G.M., 2021. Leachability of metals from waste incineration residues by iron- and sulfur-oxidizing bacteria. J. Environ. Manag. 280, 111734 https://doi.org/10.1016/j.jenvman.2020.111734.

Ma, N., 2016. Recycling of basic oxygen furnace steelmaking dust by in-process separation of zinc from the dust. J. Clean. Prod. 112, 4497–4504. https://doi.org/10.1016/j.jclepro.2015.07.009.

Ma, N.Y., 2008. On the separation of zinc from dust in ironmaking and steelmaking off-gas cleaning systems. TMS Annu. Meet. 547–552.

Di Maria, A., Van Acker, K., 2018. Turning industrial residues into resources: an environmental impact assessment of goethite valorization. Engineering 4, 421–429. https://doi.org/10.1016/j.eng.2018.05.008.

Mishra, D., Kim, D.-J., Ahn, J.-G., Rhee, Y.-H., 2005. Bioleaching: a microbial process of metal recovery. A rev., Met. Mater. Int. 11, 249–256. https://doi.org/10.1007/bf03027450.

Mishra, D., Kim, D.J., Ralph, D.E., Ahn, J.G., Rhee, Y.H., 2008. Bioleaching of spent hydro-processing catalyst using acidophilic bacteria and its kinetics aspect. J. Hazard Mater. 152, 1082–1091. https://doi.org/10.1016/j.jhazmat.2007.07.083.

Mo, X., Li, X., Wen, J., 2019. Optimization of bioleaching of fluoride-bearing uranium ores by response surface methodology. J. Radioanal. Nucl. Chem. 321, 579–590. https://doi.org/10.1007/s10967-019-06594-7.

Moazzam, P., Boroumand, Y., Rabiei, P., Baghbaderani, S.S., Mokarian, P., Mohagheghian, F., Mohammed, L.J., Razmjou, A., 2021. Lithium bioleaching: an emerging approach for the recovery of Li from spent lithium ion batteries. Chemosphere 277, 130196. https://doi.org/10.1016/j.chemosphere.2021.130196.

Muddanna, M.H., Baral, S.S., 2021. Bioleaching of rare earth elements from spent fluid catalytic cracking catalyst using *Acidothiobacillus ferrooxidans*. J. Environ. Chem. Eng. 9, 104848 https://doi.org/10.1016/j.jece.2020.104848.

Naseri, T., Bahaloo-Horeh, N., Mousavi, S.M., 2019. Bacterial leaching as a green approach for typical metals recovery from end-of-life coin cells batteries. J. Clean. Prod. 220, 483–492. https://doi.org/10.1016/j.jclepro.2019.02.177.

Niu, Z., Huang, Q., Xin, B., Qi, C., Hu, J., Chen, S., Li, Y., 2016. Optimization of bioleaching conditions for metal removal from spent zinc-manganese batteries using response surface methodology. J. Chem. Technol. Biotechnol. 91, 608–617. https://doi.org/10.1002/jctb.4611.

Nkulu, G., Gaydardzhiev, S., Mwema, E., 2013. Statistical analysis of bioleaching copper, cobalt and nickel from polymetalic concentrate originating from Kamoya deposit in the Democratic Republic of Congo. Miner. Eng. 48, 77–85. https://doi.org/10.1016/j.mineng.2012.10.007.

Opara, C.B., Blannin, R., Ebert, D., Frenzel, M., Pollmann, K., Kutschke, S., 2022. Bioleaching of metal(loid)s from sulfidic mine tailings and waste rock from the Neves Corvo mine, Portugal, by an acidophilic consortium. Miner. Eng. 188, 107831 https://doi.org/10.1016/J.MINENG.2022.107831.

Pathak, A., Srichandan, H., Kim, D.J., 2019. Column bioleaching of metals from refinery spent catalyst by *Acidithiobacillus thiooxidans*: effect of operational modifications on metal extraction, metal precipitation, and bacterial attachment. J. Environ. Manag. 242, 372–383. https://doi.org/10.1016/j.jenvman.2019.04.081.

Pedram, H., Hosseini, M.R., Bahrami, A., 2020. Utilization of *A. niger* strains isolated from pistachio husk and grape skin in the bioleaching of valuable elements from red mud. Hydrometallurgy 198, 105495. https://doi.org/10.1016/j.hydromet.2020.105495.

Pirsaheb, M., Zadsar, S., Hossini, H., Omid Rastegar, S., Kim, H., 2022. Bioleaching of carbide waste using spent culture of Acidithiobacillus bacteria: effective factor evaluation and ecological risk assessment. Environ. Technol. Innovat. 28, 102801 https://doi.org/10.1016/j.eti.2022.102801.

Pourhossein, F., Mousavi, S.M., 2019. A novel step-wise indirect bioleaching using biogenic ferric agent for enhancement recovery of valuable metals from waste light emitting diode (WLED). J. Hazard Mater. 378, 120648 https://doi.org/10.1016/j.jhazmat.2019.05.041.

Rastegar, S.O., Mousavi, S.M., Shojaosadati, S.A., Sarraf Mamoory, R., 2015. Bioleaching of V, Ni, and Cu from residual produced in oil fired furnaces using *Acidithiobacillus ferrooxidans*. Hydrometallurgy 157, 50–59. https://doi.org/10.1016/j.hydromet.2015.07.006.

Rawlings, D.E., Johnson, D.B., 2007. Biomining. Springer Berlin, Heidelberg, p. 314. https://doi.org/10.1007/978-3-540-34911-2.

Riley, A.L., MacDonald, J.M., Burke, I.T., Renforth, P., Jarvis, A.P., Hudson-Edwards, K.A., McKie, J., Mayes, W.M., 2020. Legacy iron and steel wastes in the UK: extent, resource potential, and management futures. J. Geochem. Explor. 219, 106630 https://doi.org/10.1016/j.gexplo.2020.106630.

Roberts, M., Srivastava, P., Webster, G., Weightman, A.J., Sapsford, D.J., 2023. Biostimulation of jarosite and iron oxide-bearing mine waste enhances subsequent metal recovery. J. Hazard Mater. 445, 130498 https://doi.org/10.1016/j.jhazmat.2022.130498.

Rodriguez Rodriguez, N., Machiels, L., Onghena, B., Spooren, J., Binnemans, K., 2020. Selective recovery of zinc from goethite residue in the zinc industry using deep-eutectic solvents. In: Royal Society of Chemistry, pp. 7328–7335. https://doi.org/10.1039/D0RA00277A, 10.

Roy, J.J., Madhavi, S., Cao, B., 2021. Metal extraction from spent lithium-ion batteries (LIBs) at high pulp density by environmentally friendly bioleaching process. J. Clean. Prod. 280, 124242 https://doi.org/10.1016/j.jclepro.2020.124242.

Srichandan, H., Mohapatra, R.K., Parhi, P.K., Mishra, S., 2019. Bioleaching approach for extraction of metal values from secondary solid wastes: a critical review. Hydrometallurgy 189, 105122. https://doi.org/10.1016/j.hydromet.2019.105122.

Srichandan, H., Mohapatra, R.K., Singh, P.K., Mishra, S., Parhi, P.K., Naik, K., 2020. Column bioleaching applications, process development, mechanism, parametric effect and modelling: a review. J. Ind. Eng. Chem. 90, 1–16. https://doi.org/10.1016/j.jiec.2020.07.012.

Stewart, D.J.C., Barron, A.R., 2020. Pyrometallurgical removal of zinc from basic oxygen steelmaking dust – a review of best available technology. Resour. Conserv. Recycl. 157, 104746 https://doi.org/10.1016/J.RESCONREC.2020.104746.

Stewart, D.J.C., Scrimshire, A., Thomson, D., Bingham, P.A., Barron, A.R., 2022. The chemical suitability for recycling of zinc contaminated steelmaking by-product dusts: the case of the UK steel plant, Resources. Conserv. Recycl. Adv. 14, 200073 https://doi.org/10.1016/j.rcradv.2022.200073.

Tang, J., Gong, G., Su, H., Wu, F., Herman, C., 2016. Performance evaluation of a novel method of frost prevention and retardation for air source heat pumps using the orthogonal experiment design method. Appl. Energy 169, 696–708. https://doi.org/10.1016/j.apenergy.2016.02.042.

Third, K.A., Cord-Ruwisch, R., Watling, H.R., 2000. The role of iron-oxidizing bacteria in stimulation or inhibition of chalcopyrite bioleaching. Hydrometallurgy 57, 225–233. https://doi.org/10.1016/S0304-386X(00)00115-8.

Tian, B., Cui, Y., Qin, Z., Wen, L., Li, Z., Chu, H., Xin, B., 2022. Indirect bioleaching recovery of valuable metals from electroplating sludge and optimization of various parameters using response surface methodology (RSM). J. Environ. Manag. 312, 114927 https://doi.org/10.1016/j.jenvman.2022.114927.

Tezyapar Kara, I., Marsay, N., Huntington, V., Coulon, F., Alamar, M.C., Capstick, M., Higson, S., Buchanan, A., Wagland, S., 2022. Assessing metal recovery opportunities through bioleaching from past metallurgical sites and waste deposits: UK case study. Detritus 21, 62–71. https://doi.org/10.31025/2611-4135/2022.17232.

Tezyapar Kara, I., Kremser, K., Wagland, S.T., Coulon, F., 2023. Bioleaching metal-bearing wastes and by-products for resource recovery: a review. Springer. https://doi.org/10.1007/s10311-023-01611-4.

Wang, X., Sun, Z., Liu, Y., Min, X., Guo, Y., Li, P., Zheng, Z., 2019. Effect of particle size on uranium bioleaching in column reactors from a low-grade uranium ore. Bioresour. Technol. 281, 66–71. https://doi.org/10.1016/j.biortech.2019.02.065.

Yazici, H., Yardimci, M.Y., Aydin, S., Karabulut, A.Ş., 2009. Mechanical properties of reactive powder concrete containing mineral admixtures under different curing regimes. Construct. Build. Mater. 23, 1223–1231. https://doi.org/10.1016/j.conbuildmat.2008.08.003.

Zare Tavakoli, H., Abdollahy, M., Ahmadi, S.J., Khodadadi Darban, A., 2017. Kinetics of uranium bioleaching in stirred and column reactors. Miner. Eng. 111, 36–46. https://doi.org/10.1016/j.mineng.2017.06.003.

Zeng, G., Luo, S., Deng, X., Li, L., Au, C., 2013. Influence of silver ions on bioleaching of cobalt from spent lithium batteries. Miner. Eng. 49, 40–44. https://doi.org/10.1016/j.mineng.2013.04.021.